Novel Iron(III) Complexes of Tripodal and Linear Tetradentate Bis(phenolate) Ligands: Close Relevance to Intradiol-Cleaving Catechol Dioxygenases

ARTICLE *in* INORGANIC CHEMISTRY · JANUARY 2004

Impact Factor: 4.76 · DOI: 10.1021/ic020569w · Source: PubMed

4 AUTHORS, INCLUDING:

R. Srinivasa Gopalan
Unilever
24 PUBLICATIONS **581** CITATIONS
SEE PROFILE

Giridhar U Kulkarni
Centre for Nano and Soft Matter Sciences
271 PUBLICATIONS **4,439** CITATIONS
SEE PROFILE

Inorg. Chem. **2003**, *42*, 8283–8293

Novel Iron(III) Complexes of Tripodal and Linear Tetradentate Bis(phenolate) Ligands: Close Relevance to Intradiol-Cleaving Catechol Dioxygenases

Marappan Velusamy and Mallayan Palaniandavar*

Department of Chemistry, Bharathidasan University, Tiruchirappalli 620 024, India

R. Srinivasa Gopalan and G. U. Kulkarni

Chemistry and Physics of Materials Unit, Jawaharlal Nehru Center for Advanced Scientific Research, Bangalore 560 064, India

Received September 18, 2002

Four new iron(III) complexes of the bis(phenolate) ligands *N*,*N*-dimethyl-*N*′,*N*′-bis(2-hydroxy-3,5-dimethylbenzyl)-ethylenediamine [H_2(L1)], *N*,*N*-dimethyl-*N*′,*N*′-bis(2-hydroxy-4-nitrobenzyl)ethylenediamine [H_2(L2)], *N*,*N*′-dimethyl-*N*,*N*′-bis(2-hydroxy-3,5-dimethylbenzyl)ethylenediamine [H_2(L3)], and *N*,*N*′-dimethyl-*N*,*N*′-bis(2-hydroxy-4-nitrobenzyl)-ethylenediamine [H_2(L4)] have been isolated and studied as structural and functional models for the intradiol-cleaving catechol 1,2-dioxygenases (CTD). The complexes [Fe(L1)Cl] (**1**), [Fe(L2)(H_2O)Cl] (**2**), [Fe(L3)Cl] (**3**), and [Fe(L4)(H_2O)Cl] (**4**) have been characterized using absorption spectral and electrochemical techniques. The single-crystal X-ray structures of the ligand H_2(L1) and the complexes **1** and **2** have been successfully determined. The tripodal ligand H_2(L1) containing a N_2O_2 donor set represents the metal-binding region of the iron proteins. Complex **1** contains an FeN_2O_2Cl chromophore with a novel trigonal bipyramidal coordination geometry. While two phenolate oxygens and an amine nitrogen constitute the trigonal plane, the other amine nitrogen and chloride ion are located in the axial positions. In contrast, **2** exhibits a rhombically distorted octahedral coordination geometry for the FeN_2O_3-Cl chromophore. Two phenolate oxygen atoms, an amine nitrogen atom, and a water molecule are located on the corners of a square plane with the axial positions being occupied by the other nitrogen atom and chloride ion. The interaction of the complexes with a few monodentate bases and phenolates and differently substituted catechols have been investigated using absorption spectral and electrochemical methods. The effect of substituents on the phenolate rings on the electronic spectral features and Fe^{III}/Fe^{II} redox potentials of the complexes are discussed. The interaction of the complexes with catecholate anions reveals changes in the phenolate to iron(III) charge-transfer band and also the appearance of a low-energy catecholate to iron(III) charge-transfer band similar to catechol dioxygenase–substrate complexes. The redox behavior of the 1:1 adducts of the complexes with 3,5-di-*tert*-butylcatechol (H_2DBC) has been also studied. The reactivities of the present complexes with H_2DBC have been studied and illustrated. Interestingly, only **2** and **4** catalyze the intradiol-cleavage of H_2DBC, the rate of oxygenation being much faster for **4**. Also **2**, but not **4**, yields an extradiol cleavage product. The reactivity of the complexes could be illustrated not on the basis of the Lewis acidity of the complexes alone but by assuming that the product release is the rate-determining phase of the catalytic reaction.

Introduction

Mono- and binuclear non-heme iron centers are frequently present in a variety of protein systems that perform important biological functions involving dioxygen.[1−4] The mononuclear non-heme iron proteins that catalyze the oxidative cleavage[5] of catechol or its derivatives with the incorporation of molecular oxygen are exemplified by catechol dioxygenases. The oxidative cleavage of catechol and other dihydroxy aromatics is a key step in the biodegradation by soil bacteria of naturally occurring aromatic molecules and many aromatic environmental pollutants.[6] If two of the hydroxyl substituents

* To whom correspondence should be addressed. E-mail: palani51@sify.com.

10.1021/ic020569w CCC: $25.00
Published on Web 11/13/2003

in the catechol substrate are in the ortho positions, then the ring cleavage can occur either between the two groups (intradiol) or between one hydroxyl group and an adjacent carbon atom (extradiol).[7] The X-ray crystal structure of the intradiol cleaving protocatechuate 3,4-dioxygenase (PCD) from *Pseudomonas putida* reveals a trigonal bipyramidal iron(III) site with four endogenous protein ligands (Tyr408, Tyr447, His460, and His462) and a solvent derived ligand.[8] A very similar active site has been found[9] very recently for another member of the intradiol dioxygenase family, namely, catechol 1,2-dioxygenase (CTD).

Several iron(III) complexes have been synthesized and studied[10−14] as models for the intradiol cleaving enzymes. However, models that mimic both the catalytic activity and spectral behavior of the iron site in these enzymes are scarce. From the point of view of models for dioxygenases, a fundamental work by Funabiki et al. on the catalytic intra- and extradiol oxygenations of 3,5-di-*tert*-butylcatechol ($DBCH_2$) by a py/bipy/$FeCl_3$ complex appeared.[15−17] In early studies Que and co-workers[18−20] synthesized a series of nitrogen-, carboxylate-, and phenolate-containing iron(III) complexes, the catalytic properties of which have been explored. Indeed they found a clear relationship between the reactivity of the adducts and Lewis acidity of the iron(III) centers as modulated by the tripodal ligand, which plays an important role in dictating the catecholate-to-iron(III) charge-transfer absorptions occurring in the visible region. Also knowledge of the rich chemistry of the iron−phenolato complexes[10−14] facilitated the elucidation of the novel substrate activation mechanism of the dioxygenase enzymes. Krebs et al.[11,13,21,22] have used a variety of nitrogen-containing tripodal ligands to obtain iron(III) model complexes. However, to date the iron(III)−salen catecholate model complex [H_2salen = *N*,*N*-bis(salicylidene)ethane-1,2-diamine] reported by Que et al.[23,24] is the only structurally known example containing two coordinated phenolate groups. Recently, we have been interested in iron(III) complexes of tri- and tetradentate ligands with one or two phenolate[25,26] donors as structural and functional models for non-heme iron proteins. Spectral and electrochemical properties of these complexes have been studied to illustrate their dioxygenase activity. We have now designed a series of new tetradentate tripodal and linear ligands containing two phenolates (Chart 1) and synthesized their nonplanar iron(III) chelates to more

Chart 1

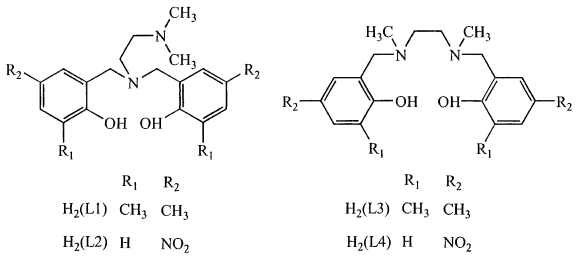

(1) (a) Solomon, E. I. *Inorg. Chem*. **2001**, *40*, 3656. (b) Que, L., Jr.; Ho, R. Y. N.*Chem. Rev.* **1996**, *96*, 2607. (c) Feig, A. L.; Lippard, S. J. *Chem. Rev*. **1994**, *94*, 759.
(2) (a) Solomon, E. I.; Brunold, T. C.; Davis, M. I.; Kemsley, J. N.; Lee, S. K.; Lehnert, N.; Neese, F.; Skulan, A. J.; Yang, Y. S.; Zhou, J. *Chem. Rev.* **2000**, *100*, 235. (b) Du Bois, J.; Mizoguchi, T. J.; Lippard, S. J. *Coord. Chem. Rev*. **2000**, *200*−*202*, 443. (c) Que, L., Jr.; Heistand, R. H., II; Mayer, R.; Roe, A. L. *Biochemistry* **1980**, *19*, 2588.
(3) (a) Chen, K.; Costas, M.; Que, L., Jr. *J. Chem. Soc., Dalton Trans*. **2002**, 672. (b) Merkx, M.; Kopp, D. A.; Sazinsky, M. H.; Blazyk, J. L.; Muller, J.; Lippard, S. J. *Angew. Chem., Int. Ed.* **2001**, *40*, 2782. (c) Que, L., Jr.; Dong, Y. *Acc. Chem. Res.* **1996**, *29*, 190. (d) Heistand, R. H., II; Laufer, R. B.; Fikrig, E.; Que, L., Jr. *J. Am. Chem. Soc.* **1982**, *104*, 2789.
(4) (a) Bugg, T. D. H. *Curr. Opin. Chem. Biol.* **2001**, *5*, 550. (b) Feeney, R. E.; Komatsu, S. S. *Struct. Bonding* (*Berlin*) **1996**, *1*, 149. (c) Ainscough, E. W.; Gainsford, A. R. *Inorg. Chem*. **1980**, *19*, 3655.
(5) (a) Lange, S. J.; Que, L., Jr. *Curr. Opin. Chem. Biol.* **1998**, *2*, 159. (b) *Microbial Degradation of Organic Molecules*; Gibson, D. T., Ed.; Marcel Dekker: New York, 1984; p 535.
(6) (a) Bugg, T. D. H.; Winfield, C. J. *Nat. Prod. Rep*. **1998**, *15*, 513. (b) Reineke, W.; Knackmuss, M. J. *Annu. Rev. Microbiol*. **1988**, *42*, 263. (c) Dagley, S. *Essays Biochem*. **1975**, *11*, 81.
(7) (a) Que, L., Jr.; Reynolds, M. F. *Met. Ions Biol. Syst.* **2000**, *37*, 505. (b) Hayaishi, O.; Katagiri, M.; Rothberg, S. *J. Am. Chem. Soc.* **1955**, *77*, 5450. (c) Kojima, Y.; Itada, N.; Hayaishi, O. *J. Biol. Chem*. **1961**, *236*, 2223. (d) Hayaishi, O. *Bacteriol. Rev.* **1966**, *30*, 720.
(8) (a) Ohlendorf, D. H.; Lipscomb, J. D.; Weber, P. C. *Nature* **1988**, *336*, 403. (b) Ohlendorf, D. H.; Orville, A. M.; Lipscomb, J. D. *J. Mol. Biol*. **1994**, *244*, 586. (c) Vetting, M. W.; Earhart, C. A.; Ohlendorf, D. H. *J. Mol. Biol*. **1994**, *236*, 372.
(9) Vetting, M. W.; Ohlendorf, D. H. J. *Structure* **2000**, *8*, 429.
(10) (a) Yamahara, R.; Ogo, S.; Masuda, H.; Watanabe, Y. *J. Inorg. Biochem*. **2002**, *88*, 284. (b) Ogo, S.; Yamahara, R.; Funabiki, T.; Masuda, H.; Watanabe, Y. *Chem. Lett*. **2001**, 1062. (c) Funabiki, T.; Fuki, A.; Hitomi, Y.; Higuchi, M.; Yamamoto, T.; Tanaka, T.; Tani, F.; Naruta, Y. *J. Inorg. Biochem*. **2002**, *91*, 151. (d) Bugg, T. D. H.; Lin, G. *J. Chem. Soc., Chem. Commun*. **2001**, 941.
(11) Pascaly, M.; Duda, M.; Rompel, A.; Sift, B. H.; Klaucke, W. M.; Krebs, B. *Inorg. Chim. Acta* **1999**, *291*, 289.
(12) (a) Mialane, P.; Tehertanov, L.; Banse, F.; Sainton, J.; Girerd, J.-J. *Inorg. Chem*. **2000**, *39*, 2440. (b) Mialane, P.; Girerd, J.-J.; Guilhem, J.; Tehertanov, L. *Inorg. Chim. Acta* **2000**, *298*, 38.
(13) Pascaly, M.; Nazikkol, C.; Schweppe, F.; Wiedemann, A.; Zurlinden, K.; Krebs, B. *Z. Anorg. Allg. Chem.* **2000**, *626*, 50.
(14) (a) Gang, L.; Reid, G.; Bugg, T. D. H. *J. Chem. Soc., Chem. Commun*. **2000**, 1119. (b) Yoon, S.; Lee, H.-J.; Lee, K.-B.; Jang, H. G. *Bull. Korean Chem. Soc.* **2000**, *21*, 923. (c) Ogihara, T.; Hikichi, S.; Akita, M.; Moro-oka, Y. *Inorg. Chem*. **1998**, *37*, 2614. (d) Jang, H. G.; Cox, D. D.; Que, L., Jr. *J. Am. Chem. Soc.* **1991**, *113*, 9200.
(15) Funabiki, T.; Mizoguchi, A.; Sugimoto, T.; Yoshida, S. *Chem. Lett.* **1983**, 917.
(16) Funabiki, T.; Mizoguchi, A.; Sugimoto, T.; Tada, S.; Tsuji, M.; Sakamoto, H.; Yoshido, S. *J. Am. Chem. Soc.* **1986**, *108*, 2921.
(17) (a) Funabiki, T.; Ishikawa, M.; Nagai, Y.; Yorita, J.; Yoshida, S. *J. Chem. Soc., Chem. Commun*. **1994**, 1951. (b) Funabiki, T.; Yoneda, I.; Ishikawa, M.; Ujiie, M.; Nagai, Y.; Yoshida, S. *J. Chem. Soc., Chem. Commun*. **1994**, 1453. (c) Funabiki, T.; Sakamoto, H.; Yoshida, S.; Tarama, K. *J. Chem. Soc., Chem. Commun*. **1979**, 754. (d) Funabiki, T.; Tada, S.; Yoshioka, T.; Takano, M.; Yoshida, S. *J. Chem. Soc., Chem. Commun*. **1986**, 1699. (e) Funabiki, T.; Konishi, T.; Kobayashi, S.; Mizoguchi, A.; Takano, M.; Yoshida, S. *Chem. Lett.* **1987**, 719.
(18) Cox, D. D.; Benkovic, S. J.; Bloom, L. M.; Bradley, F. C.; Nelson, M. J.; Que, L., Jr.; Wallick, D. E. *J. Am. Chem. Soc.* **1988**, *110*, 2026.
(19) Cox, D. D.; Que, L., Jr. *J. Am. Chem. Soc.* **1988**, *110*, 8085.
(20) Que, L., Jr.; Kolanczyk, R. C.; White, L. S. *J. Am. Chem. Soc.* **1987**, *109*, 5373.
(21) Duda, M.; Pascaly, M.; Krebs, B. *J. Chem. Soc., Chem. Commun*. **1997**, 835.
(22) Pascaly, M.; Duda, M.; Schweppe, F.; Zurlinden, K.; Müller, F. K.; Krebs, B. *J. Chem. Soc., Dalton Trans.* **2001**, 828.
(23) Lauffer, R. B.; Heistand, R. H., II; Que, L., Jr. *Inorg. Chem*. **1983**, *22*, 50.
(24) (a) Heistand, R. H., II; Randall, B.; Fikrig, E.; Que, L., Jr. *J. Am. Chem. Soc.* **1982**, *104*, 2789. (b) Heistand, R. H., II; Lawrenceroe, A.; Que, L., Jr. *Inorg. Chem.* **1982**, *21*, 676.
(25) (a) Palaniandavar, M.; Viswanathan, R. *Proc. Indian Acad. Sci., Chem. Sci.* **1996**, *108*, 235. (b) Viswanathan, R.; Palaniandavar, M.; Balasubramanian, T.; Muthiah, T. P. *J. Chem. Soc., Dalton Trans*. **1996**, 2519. (c) Viswanathan, R.; Palaniandavar, M. *J. Chem. Soc., Dalton Trans*. **1995**, 1259.
(26) Viswanathan, R.; Palaniandavar, M.; Balasubramanian, T.; Muthiah, T. P. *Inorg. Chem.* **1998**, *37*, 2943.

Chart 2

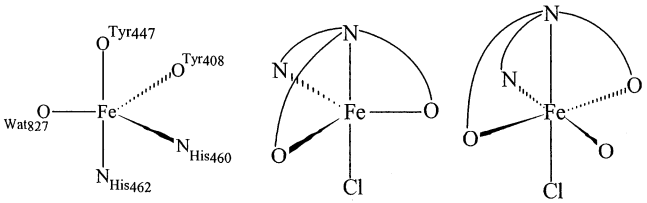

Chart 3

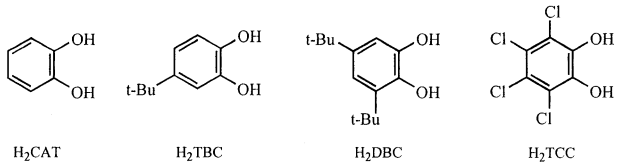

closely mimic the non-heme iron(III) coordination environment, substrate interaction, and chemistry of the catalytic cycle of these enzymes. The structural, spectral, and electrochemical characterization of all the complexes are discussed with a particular view toward evaluating the influence of coordination of two phenolates and sterically hindered tertiary amine nitrogen and variation in the phenolate ring substituents.

In this report are discussed the X-ray crystal structures of a N_2O_2 ligand and two bis(phenolato)iron(III) model complexes. One of the latter two complexes is a rare example of a monomeric iron(III) complex [Fe(L1)Cl] (**1**) with trigonal bipyramidal geometry (Chart 2), formed by the tetradentate tripodal bis(phenolato) ligand *N*,*N*-dimethyl-*N*′,*N*′-bis(2-hydroxy-3,5-dimethylbenzyl)ethylenediamine [H_2(L1)]. The only other example reported by Fujii et al.[27] is [Fe(L)(H_2O)]-ClO_4, where L is the sterically bulky Schiff base ligand bis-(3,5-dimesitylsalicylidene)-1,2-dimesitylethylenediamine. A comparison of the coordinatively unsaturated complex **1** with the octahedral complex [Fe(L2)(H_2O)Cl] (**2**) derived from the closely related ligand *N*,*N*-dimethyl-*N*′,*N*′-bis(2-hydroxy-4-nitrobenzyl)ethylenediamine [H_2(L2)] enables us to understand the effect of varying the substitution on phenolate ring in tuning the spectral and electrochemical properties and reactivity of the iron(III) model complexes and throw light on the enzymatic mechanism of intradiol cleavage. While **2** shows intradiol cleavage, **1** shows interesting spectral and chemical properties but no cleavage activity. The interaction of the present complexes with variously substituted catechols (Chart 3) has been also probed to understand the difference in reactivity.

Experimental Section

Materials. *N*,*N*-Dimethylethylenediamine, *N*,*N*′-dimethylethylenediamine, 3,4,5,6-tetrachlorocatechol (Lancaster), 3,5-di-*tert*-butylcatechol, 4-*tert*-butylcatechol, 2,4-dimethylphenol (Aldrich), and iron(III) chloride (anhydrous) (Merck) were used as received. The supporting electrolyte tetra-*N*-hexylammonium perchlorate (G. F. Smith) was recrystallized twice from aqueous ethanol.

Synthesis of Ligands. The ligands *N*,*N*′-dimethyl-*N*,*N*′-bis(2-hydroxy-3,5-dimethylbenzyl)ethylenediamine,[28] H_2(L3), and *N*,*N*′-dimethyl-*N*,*N*′-bis(2-hydroxy-4-nitrobenzyl)ethylenediamine,[29] H_2-(L4), were synthesized by published procedures.

***N*,*N*-Dimethyl-*N*′,*N*′-bis(2-hydroxy-3,5-dimethylbenzyl)ethylenediamine, H_2(L1)**. To aqueous formaldehyde (37%, 0.90 g, 30 mmol) cooled at 0 °C was added a solution of *N*,*N*-dimethylethylenediamine (1.76 g, 20 mmol) in methanol (30 mL) under a flow of nitrogen. To this solution was added 2,4-dimethylphenol (4.9 g, 40 mmol) in methanol (15 mL) dropwise with stirring. The solution was stirred for 72 h at about 30 °C and then refluxed for 2 h. The two layer system was left in a freezer when the oil at the bottom crystallized. The crystals were washed with methanol and dried under $CaCl_2$. Mp: 155−158 °C. Yield: 56%. ^{1}H NMR ($CDCl_3$): δ 2.25 (s, 12H, CH_3), 2.35 (s, 6H, N−CH_3), 2.55 (s, 4H, CH_2-CH_2), 3.55 (s, 4H, CH_2), 6.65 (s, 2H, aryl), 6.85 (s, 2H, aryl).

***N*,*N*-Dimethyl-*N*′,*N*′-bis(2-hydroxy-4-nitrobenzyl)ethylenediamine, H_2(L2).** This was prepared by a modification of a method reported[29] already. To a cold methanol solution (25 mL) containing *N*,*N*-dimethylethylenediamine (0.35 g, 4 mmol) and triethylamine (0.81 g, 8 mmol) was added dropwise 2-(chloromethyl)-4-nitrophenol[30] (1.5 g, 8 mmol) in tetrahydrofuran (20 mL) with rapid stirring. The mixture was allowed to warm to room temperature and then heated to reflux for 4 h. After rotaevaporation of the solvent to dryness, tetrahydrofuran (60 mL) was added to the residue and the mixture was heated to reflux. After cooling, the suspension was filtered off and the filtrate was rotaevaporated under reduced pressure to give a yellow solid. The solid was thoroughly washed with diethyl ether and then recrystallized from methanol. Mp: 175−178 °C. Yield: 70%. ^{1}H NMR (DMSO-d_6): δ 7.9−8.2 (m, 4H, aryl), 6.82−6.95 (m, 2H, aryl), 3.7 (s, 4H, CH_2), 3.05(s, 4H, CH_2-CH_2) and 2.52 (s, 6H, N−CH_3).

Preparation of Iron(III) Complexes. [Fe(L1)Cl] (1). A methanolic slurry of the ligand H_2(L1) (0.36 g, 1 mmol) was treated with anhydrous $FeCl_3$ (0.16 g, 1 mmol) in methanol (10 mL), and then triethylamine (0.20 g, 2 mmol) in methanol (5 mL) was added. The resulting blue colored solution was refluxed for 2 h and then rotaevaporated to dryness under reduced pressure. The resulting solid was dried over P_4O_{10} and recrystallized from hot acetonitrile to give dark blue X-ray-quality crystals. Yield: 0.30 g (67%). Anal. Calcd for $C_{22}H_{30}N_2O_2FeCl$: C, 59.27; H, 6.78; N, 6.28. Found: C, 59.35; H, 6.82; N, 6.3.

[Fe(L2)(H_2O)Cl] (2). To a solution of the ligand H_2(L2) (0.78 g, 2 mmol) and triethylamine (0.41 g, 4 mmol) in methanol (20 mL) was added anhydrous $FeCl_3$ (0.33 g, 2 mmol) in methanol (10 mL) with stirring. The product formed was filtered off, washed with small amounts of cold methanol, and then dried over P_4O_{10}. Crystals suitable for X-ray diffraction were obtained by vapor diffusion of diethyl ether into an acetonitrile solution of the complex. Yield: 0.29 g (58.3%). Anal. Calcd for $C_{18}H_{22}N_4O_7FeCl$: C, 43.44; H, 4.46; N, 11.26. Found: C, 43.40; H, 4.52; N, 11.24.

[Fe(L3)Cl] (3). Triethylamine (0.10 g, 1 mmol) and H_2(L3) (0.39 g, 1 mmol) were dissolved in methanol (25 mL). To this solution was added anhydrous $FeCl_3$ (0.163 g, 1 mmol) in methanol (10 mL) and heated at reflux for 2 h. After cooling, the resulting solution was filtered to remove residual solids. The filtrate was then rotaevaporated to dryness. The blue powder obtained was recrystallized from a hot mixture of dichloromethane and hexane (1:1) and

(27) Fujii, H.; Funahashi, Y. *Angew. Chem., Int. Ed.* **2002**, *41*, 3638.

(28) Mialane, P.; Anzolabehere-Mallart, E.; Blondin, G.; Nivorojkine, A.; Guilhem, J.; Tcheratanova, L.; Cesario, M.; Ravi, N.; Bominaar, E.; Girerd, J.-J.; Munck, E. *Inorg. Chim. Acta* **1997**, *263*, 367.

(29) Wong, Y.-L.; Yan, Y.; Chan, E. S. H.; Yang, Q.; Mak, T. C. W.; Ng, D. K. P. *J. Chem. Soc., Dalton Trans.* **1998**, 3057.

(30) Horning, E. C. *Organic Synthesis*; Wiley: New York, 1955; Collect. Vol. III, p 468.

dried over P_4O_{10}. Yield: 0.35 g (78.6%). Anal. Calcd for $C_{22}H_{30}N_2O_2FeCl$: C, 59.27; H, 6.78; N, 6.28. Found: C, 59.15; H, 6.65; N, 6.20.

[Fe(L4)(H$_2$O)Cl] (4). A methanolic solution (20 mL) containing the ligand H_2(L4) (0.36 g, 1 mmol), anhydrous $FeCl_3$ (0.16 g, 1 mmol), and triethylamine (0.10 g, 1 mmol) was heated to reflux for 2 h. After cooling, the solution was filtered to remove residual solids. The filtrate was then rotaevaporated to dryness. The violet-brown powder obtained was recrystallized from a hot mixture of dichloromethane−hexane (1:1) and dried over P_4O_{10}. Yield: 0.32 g (66.4%). Anal. Calcd for $C_{18}H_{20}N_4O_6FeCl$: C, 45.07; H, 4.20; N, 11.68. Found: C, 45.15; H, 4.18; N, 11.50.

Physical Measurements. Elemental analyses were performed at CDRI, Lucknow, India. The electronic spectra were recorded on a Hitachi U-3410 double-beam UV−vis−NIR spectrophotometer. Cyclic voltammetry (CV) and differential pulse voltammetry (DPV) were performed using a three-electrode cell configuration. A platinum sphere, a platinum plate, and Ag(s)/$AgNO_3$ were used as working, auxiliary, and reference electrodes, respectively. The supporting electrolyte used was NBu_4ClO_4. The platinum sphere electrode was sonicated for 2 min in dilute nitric acid, dilute hydrazine hydrate, and then in double-distilled water to remove the impurities. The temperature of the electrochemical cell was maintained at 25 ± 0.2 °C by a cryocirculator (HAAKE D8 G). Bubbling research grade nitrogen deoxygenated the solutions, and an atmosphere of nitrogen was maintained over the solution during measurements. The $E_{1/2}$ values were observed under identical conditions for various scan rates. The instruments utilized included an EG&G PAR 273 potentiostat/galvanostat and an IBM PS2 computer along with EG&G M270 software to carry out the experiments and to acquire the data. GC-MS analysis were performed using HP (Hewlett-Packard) 6890 Plus series gas chromatograph equipped with a FID detector and a HP-1 capillary column (30 m, 0.32 mm i.d) with the following temperature program: initial temperature, 200 °C (initial time, 2 min); heating rate, 2 °C min^{-1}; final temperature, 240 °C (final time, 3 min); injector temperature, 250 °C; FID detector temperature, 250 °C.

Crystallographic Data Collection and Structure Refinement. Crystals suitable for X-ray diffraction were chosen after careful examination under an optical microscope. For the crystals H_2(L1), **1**, and **2** X-ray diffraction intensities were measured by ω scans using a Siemens three-circle diffractometer attached with a CCD area detector and a graphite monochromator for the Mo Kα radiation (50 kV, 40 mA). The unit cell parameters and the orientation matrix of the crystals were initially determined using approximately 60 reflections from 25 frames collected over a small ω scan of 7.5° sliced at 0.3° interval. The details of data collection and structure analysis of **1** and **2** are given in Table 1, and those of H_2(L1), as Supporting Information. A hemisphere of reciprocal space was then collected using SMART[31] software with the 2θ setting at 28°. Data reduction was performed using the SAINT[31] program, and the orientation matrix along with the detector and cell parameters was refined for every 40 frames on all the measured reflections. An empirical absorption correction based on symmetry-equivalent reflections was applied using the SADABS[32] program taking the merged reflection file obtained from SAINT as the input. The correct Laue groups of the crystals were chosen for the absorption correction. All the structures were solved by direct methods using the SHELXS-97 program[33] and refined by the full-matrix least-squares method on F^2 using the SHELXL-93 program.[34]

Table 1. Crystal Data and Structure Refinement for [Fe(L1)Cl] (**1**) and [Fe(L2)Cl(H$_2$O)](CH$_3$CN) (**2**)

	1	**2**
chem formula	$C_{22}H_{30}ClFeN_2O_2$	$C_{40}H_{50}Cl_2Fe_2N_{10}O_{14}$
fw	445.78	1077.50
cryst system	monoclinic	triclinic
space group	$P2_1/a$	$P\bar{1}$
Mo Kα radiatn λ, Å	0.710 69	0.710 73
a, Å	7.1152(3)	8.8643(8)
b, Å	38.1460(18)	11.1566(10)
c, Å	8.5167(4)	12.3585(11)
α, deg	90	99.888(2)
β, deg	106.3044(9)	104.143(2)
γ, deg	90	90.0680(10)
V, Å^3	2218.61(17)	1166.36(18)
Z	4	2
temp, K	293(2)	293(2)
ρ(calcd), mg/m^3	1.335	1.534
μ, mm^{-1}	0.819	0.813
residuals[a] [$I > 2\sigma(I)$]		
R_1	0.0421	0.0718
wR_2	0.1167	0.2170

[a] $R = \sum||F_o| - |F_c||/\sum|F_o|$; $wR_2 = \{\sum[w(F_o^2 - F_c^2)^2/\sum[w(F_o^2)^2]\}^{1/2}$.

Table 2. Selected Bond Lengths (Å) and Bond Angles (deg) for **1** and **2**

[Fe(L1)Cl] (**1**)		[Fe(L2)Cl(H$_2$O)](CH$_3$CN) (**2**)	
Fe1−O2	1.855(2)	Fe1−O1	1.908(4)
Fe1−O1	1.868(2)	Fe1−O4	1.967(4)
Fe1−N2	2.152(2)	Fe1−O7	2.104(4)
Fe1−N1	2.288(2)	Fe1−N2	2.203(6)
Fe1−Cl1	2.29(1)	Fe1−N3	2.252(4)
		Fe1−Cl1	2.295(17)
O2−Fe1−O1	121.3(1)	O1−Fe1−O4	172.00(18)
O2−Fe1−N2	113.1(1)	O1−Fe1−O7	86.21(18)
O1−Fe1−N2	123.0(1)	O4−Fe1−O7	87.25(17)
O2−Fe1−N1	89.1(1)	O1−Fe1−N2	90.78(19)
O1−Fe1−N1	85.6(1)	O4−Fe1−N2	94.57(18)
N2−Fe1−N1	79.7(1)	O7−Fe1−N2	167.00(18)
O2−Fe1−Cl1	99.4(1)	O1−Fe1−N3	87.81(16)
O1−Fe1−Cl1	94.3(1)	O4−Fe1−N3	87.21(16)
N2−Fe1−Cl1	92.2(1)	O7−Fe1−N3	86.59(16)
N1−Fe1−Cl1	170.1(1)	N2−Fe1−N3	80.65(18)
		O1−Fe1−Cl1	95.66(13)
		O4−Fe1−Cl1	89.82(12)
		O7−Fe1−Cl1	98.12(13)
		N2−Fe1−Cl1	94.77(15)
		N3−Fe1−Cl1	174.31(12)

The positions of the hydrogen atoms were geometrically fixed. All the non-hydrogen atoms were refined anisotropically. The molecular structures were drawn using ZORTEP.[35] The selected bond length and bond angles for **1** and **2** are given in Table 2.

Reactivity Studies. Catechol 1,2-Dioxygenase Activity. The catechol-cleavage activity of the complexes toward 3,5-di-*tert*-butylcatechol (H_2DBC) was examined[11,12,21] by exposing to dioxygen a solution of the iron(III) complex−DBC adduct generated in situ by treating the complex in DMF solution (2.3×10^{-4} M) with H_2DBC (2.3×10^{-4} M) and piperidine (4.6×10^{-4} M) and monitoring the disappearance of the LMCT band at ambient temperature (25 °C). Kinetic analyses[12,36] of the intradiol cleaving reactions were carried out by time-dependent measurements of the

(31) Siemens Analytical X-ray Instruments Inc., Madison, WI, 1995.
(32) Sheldrick, G. M. *SADABS User Guide*; University of Göttingen: Göttingen, Germany, 1997.
(33) Sheldrick, G. M. *SHELXS-97: Program for the Solution of Crystal Structure*; University of Göttingen: Göttingen, Germany, 1997.
(34) Sheldrick, G. M. *SHELXL-93: Program for the Refinement of Crystal Structure*; University of Göttingen: Göttingen, Germany, 1993.
(35) Zsolnai, L. *ZORTEP, an interactive ORTEP program*; University of Heidelberg: Heidelberg, Germany, 1996.

lower energy catecholate-to-iron(III) charge-transfer band at ambient temperatures (25 °C). The solubility[37] of O_2 in DMF at 25 °C was taken as 4.86 mM.

Identification of the Dioxygenated Products. The dioxygenase activities of the present complexes were determined using a known procedure.[16,38] The complex (0.5 mmol), 3,5-di-*tert*-butylcatechol (0.5 mmol), and piperidine (1 mmol) were dissolved in DMF (10 mL) at 1 atm oxygen. After 48 h, the reaction was quenched by the addition of 2 M HCl (30 mL). Organic products were extracted from the aqueous DMF solution with diethyl ether (3 × 50 mL), dried over anhydrous Na_2SO_4, and then concentrated. The products were identified by using GC-MS analysis.

Results and Discussion

Synthesis and Characterization of Ligands and Complexes. The present ligands were synthesized according to known procedures, which involve Mannich condensation and simple substitution reactions. The diamines *N*,*N*-dimethylethylenediamine and *N*,*N*′-dimethylethylenediamine have been used as the starting materials, and the amino hydrogens in them have been replaced with different substituted phenolate moieties to generate the phenolate ligands (Chart 1) for this study. The tetradentate ligands H_2(L1) and H_2(L3) were synthesized in good yields by the reaction of the Mannich base formed in situ in the presence of paraformaldehyde with *ortho*- and *para*-substituted phenols by the method reported[28] already. The ligands H_2(L2) and H_2(L4) were synthesized by the reaction respectively of *N*,*N*-dimethylethylenediamine and *N*,*N*′-dimethylethylenediamine with 2-hydroxy-5-nitrobenzyl chloride in 1:2 ratio by the reported procedure.[29] The flexible tripodal ligands H_2(L1) and H_2(L2) are expected to form complexes with structures exhibiting a range of conformations. The secondary amine nitrogen incorporated as one of the arms in them is expected to influence the iron(III) coordination structures as well as the electronic properties of the complexes. The linear tetradentate ligands H_2(L3) and H_2(L4) with sterically hindered *N*,*N*′-dimethyl-substituted amine nitrogens and two 2,4-disubstituted phenol arms may be expected to favor monomeric octahedral complexes but with varying structural, spectral, and electrochemical properties. The nitro and methyl substituents have been introduced not only to tune the spectral and electrochemical properties but also to vary the reactivity of the model complexes. While **1** and **3** are formulated as monomeric [FeLCl], **2** and **4** are formulated as monomeric [FeLCl(H_2O)], which is supported by the X-ray crystal structures of **1** and **2** (cf. below). The conductivities of all the complexes (Λ_M, 85−95 Ω^{-1} cm^2 mol^{-1}) suggest that the chloride ions are quite certainly not coordinated in methanol solution. So complex **2**, which contains two readily replaceable cis coordination sites, is convenient for studying the effect of substrate adduct formation on spectra. The five-coordinated complexes **1** and **3** containing only one coordinated chloride ion may expand their coordination sphere to accommodate bidentate substrate molecules. All the iron(III) complexes have magnetic moments in the range 5.6−5.8 μ_B at room temperature, consistent with a high-spin ferric center with five unpaired electrons. The catecholate adducts of the iron(III) chloride complexes were generated in solution for spectral and reactivity studies.

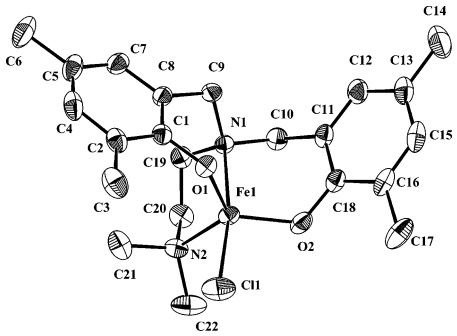

Figure 1. ZORTEP drawing of [Fe(L1)Cl] (**1**), showing the atom numbering scheme and the thermal motion ellipsoids (50% probability level) for the non-hydrogen atoms.

Description of the X-ray Crystal Structures. Structure of [Fe(L1)Cl] (1). The ZORTEP plot of the complex is illustrated in Figure 1 with atom numbering scheme. The selected bond lengths and bond angles are given in Table 2. The coordination environment around the iron atom in **1** is described as distorted trigonal bipyramidal. The metal is bonded to two phenolate oxygens (O1, O2) and the amine nitrogen (N2) of the tripodal ligand, which define the trigonal plane of the bipyramid, and the other amine nitrogen (N1) and chloride ion occupy the apical sites. The observed Fe−O bond distances (Fe−O1, 1.867; Fe−O2, 1.855 Å) in **1** are shorter than the average octahedral Fe−O bond distance[23,25,39−41] of 1.92 Å implying relatively strong iron−oxygen overlap, which is consistent with the lower coordination number. The short Fe−O bond distance is in accordance with the high molar absorptivity of the LMCT band (cf. below). The Fe−Cl distance (2.291 Å) is in the same range[40,41] as those in octahedral iron(III) complexes suggesting that the chloride ion should be labile in solution. The Fe−N_{amine} distances (2.152, 2.288 Å) are also similar to the octahedral Fe^{III}−N distance[25,39−41] of ∼2.15 Å. The apical nitrogen is bound to iron(III) more strongly than the pendant nitrogen. The iron atom is displaced 0.178 Å above the NO_2 mean plane. The Fe−O−C bond angles (Fe−O1−C1, 122.05°; Fe−O2−C18, 122.15°) are much less than those in octahedral iron(III) complexes of phenolate ligands (∼128.5°) but are closer to the ideal value of 120° for sp^2-

(36) Yamahara, R.; Ogo, S.; Watanabe, Y.; Funabiki, T.; Jitsukawa, K.; Masuda, H.; Einaga, H. *Inorg. Chim. Acta* **2000**, *300*−*302*, 587.
(37) *Japan Chemical Society, Kagaku-Binran Basic Part II*, 2nd ed.; Maruzen: Tokyo, 1975.
(38) Weiner, H.; Hayashi, Y.; Finke, R. G. *Inorg. Chim. Acta* **1999**, *291*, 426.
(39) (a) Ainscough, E. W.; Brodie, A. M.; Plowman, J. E.; Brown, K. L.; Addison, A. W.; Gainsford, A. R. *Inorg. Chem.* **1980**, *19*, 3655. (b) Davis, J. C.; Kung, W. S.; Averill, B. A. *Inorg. Chem.* **1986**, *25*, 394. (c) Yan, S.; Que, L., Jr.; Taylor, L. F.; Anderson, O. P. *J. Am. Chem. Soc.* **1988**, *110*, 5222. (d) Clarke, E. T.; Martell, A. E.; Reibenspies, J. *Inorg. Chim. Acta* **1992**, *196*, 177. (e) Malfant, I.; Morgenstern-Badarau, I.; Philoche-Lavisalles, M.; Lloret, F. *J. Chem. Soc., Chem. Commun*. **1990**, 1338.
(40) Merkel, M.; Muller, F. K.; Krebs, B. *Inorg. Chim. Acta* **2002**, *337*, 308.
(41) McDevitt, M. R.; Addision, A. W.; Sinn, E.; Thompson, L. K. *Inorg. Chem*. **1990**, *29*, 3425.

hybridized phenolate oxygen atom suggesting that the latter interacts[41] more strongly with a half-filled dπ* orbital in iron(III) in the present complexes. The coordination geometry around iron(III) is trigonal bipyramidal with the trigonality index[42] τ of 0.79 [$\tau = (\beta-\alpha)/60$, where β represents N1−Fe−Cl1 = 170.14° and α represents O1−Fe−N2 = 123.05°; for perfect square pyramidal and trigonal bipyramidal geometries the τ values are zero and unity respectively]. Interestingly, this coordination environment is closely related to the trigonal bipyramidal metal core[8] (τ, 0.44) in the substrate-free 3,4-PCD enzyme; however, both the phenolates are equatorial in **1**, while they are mixed axial−equatorial in the enzyme active site. Complex **1** is only the second example of a structurally characterized five-coordinated trigonal bipyramidal iron(III) complex with a tetradentate ligand. The first example reported by Fujii et al.,[27] viz. [Fe(L)(H_2O)]ClO_4 (cf. above), also possesses a trigonal bipyramidal geometry (τ, 0.48) but with two mixed axial−equatorial Fe−O(phenolate)/Fe−N bonds (Fe−O, 1.863, 1.876 Å; Fe−N, 2.060, 2.084 Å) and a coordinated water molecule (Fe−O, 2.009 Å) in the trigonal plane, similar to the active site of 3,4-PCD enzyme; however, the chloride analogue [Fe(L)Cl] possesses a five-coordinated square-pyramidal geometry[27] (Fe−O, 1.881, 1.878 Å; Fe−N, 2.087, 2.102 Å; Fe−Cl, 2.234 Å). Interestingly, the Fe−O bond distances in these two complexes and in **1** are similar to those in 3,4-PCD enzyme [Fe−O(Tyr447), 1.90 Å; Fe−O(Tyr408), 1.81 Å]; however, the Fe−N bonds in them are shorter than those in the enzyme [Fe−N(His460), 2.33 Å; Fe−N(His462), 2.26 Å]. Further, only two other five-coordinate trigonal bipyramidal complexes but of bidentate ligands, [Fe(SANE)$_2$Cl][43] [H(SANE) = *N*-(2-phenylethyl)salicylideneimine, τ, 1.00] and [Fe(HBT)$_2$Br][44] [H(HBT) = 2,2′-(hydroxyphenyl)benzothiazole, τ, 0.92] are known in the literature. A similar or square-pyramidal five-coordinate geometry is suggested for **3**. But it is unfortunate that no X-ray-quality crystals could be obtained.

Structure of [Fe(L2)(H_2O)Cl] (2). The ZORTEP plot of the complex is illustrated in Figure 2 with atom numbering scheme. The selected bond lengths and bond angles are given in Table 2. Thus, the complex exhibits a six-coordinated distorted octahedral coordination geometry constituted by two trans-coordinated phenolate oxygen atoms (O1, O4) and the cis-coordinated amine nitrogen atoms (N2, N3) of the tetradentate ligand. One water molecule (O7) and a chloride ion occupy the remaining cis positions. The latter two cis coordination sites may be available for coordination of two monodentate or one bidentate base molecule like DBC^{2-}. This is relevant to the 4-HBA-PCD complex[45] (4-HBA = 4-hydroxybenzoate), in which HBA is bound in a chelated doubly deprotonated form. The trans-disposed Fe−O(phenolate) bonds are significantly different (Fe−O1, 1.890; Fe−O4, 1.993 Å) but are similar to those in the previously reported[25,39−41,46] six-coordinated iron(III) complexes. This indicates the ability of the tripodal ligand to impose a difference in Fe−O bond lengths inspite of the similarity in the phenolate oxygen atoms. This is interesting because the difference in the two Fe−tyrosinate bonds in the 3,4-PCD enzyme is thought to influence the asymmetric binding[47] of the chelated substrate moiety. Similarly, the Fe−Cl (2.291 Å) and Fe−N_{amine} (2.219, 2.248 Å) bond distances also fall in the range found in other similar octahedral iron(III) phenolate complexes.[25,39−41] The Fe−O−C bond angles (Fe−O1−C1, 135.3°; Fe−O4−C14, 135.6°) are greater than those in **1** and other octahedral iron(III) complexes of phenolate ligands (~128.5°) indicating that the sp^2-hybridized phenolate oxygens in complex **2** would interact less strongly with a half-filled dπ* orbital in iron(III)[41] than in **1,** and thus, the Fe−O(phenolate) bond distances are longer in **2** than in **1**. However, the Fe−N_{amine} distances are shorter in **2** than in **1**. Thus, the coordination environment around iron(III) in **2** is quite different[48] from that in **1**, obviously due to the difference in phenolate substitution in the ligands; the dimethyl substituents on the phenolate moieties in **1** appear to provide no steric hindrance[27] as revealed by space-filling models but electronic effects to stabilize the Fe−O(phenolate) coordination and hence the trigonal bipyramidal coordination geometry.

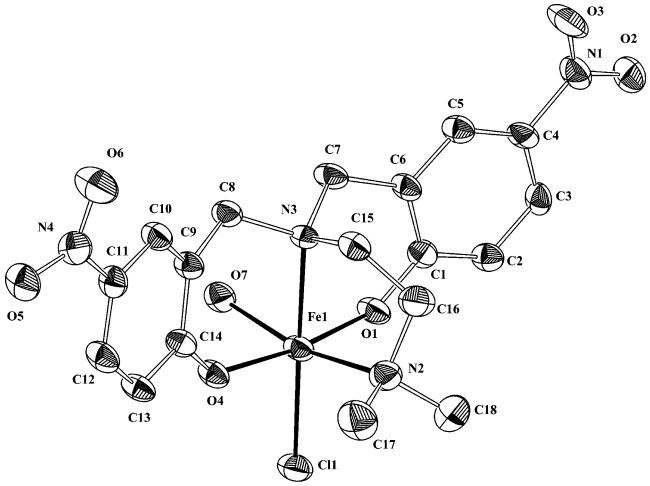

Figure 2. ZORTEP drawing of [Fe(L2)Cl(H_2O)] (**2**), showing the atom numbering scheme and the thermal motion ellipsoids (50% probability level) for the non-hydrogen atoms.

(42) Addison, A. W.; Rao, T. N.; Reedijk, J.; Van Rijn, J.; Vershcoor, G. C. *J. Chem. Soc., Dalton Trans.* **1984**, 1349. $\tau = (\beta-\alpha)/60$, where β = O1−Fe−N2 = 123.05(9)° and α = O1−Fe−N2 = 123.0(9)°; for perfect square pyramidal and trigonal bipyramidal geometries, the τ values are zero and unity, respectively.

(43) Magurany, C. J.; Strouse, C. E. *Inorg. Chem.* **1982**, *21*, 2348.

(44) Pyrz, J. W.; Pan, X.; Britton, D.; Que, L., Jr. *Inorg. Chem.* **1991**, *30*, 3461.

(45) Jo, D. H.; Que, L., Jr. *Angew. Chem., Int. Ed.* **2000**, *39*, 4284.

(46) (a) Shyu, H. L.; Wei, H. H.; Lee, G. H.; Wang, Y. *J. Chem. Soc., Dalton Trans.* **2000**, 915. (b) Lubben, M.; Meetsman, A.; Bolhuis, F.; Feringa, B. L. *Inorg. Chim. Acta* **1994**, *215*, 123. (c) Setyawati, I. A.; Rettig, S. J.; Orvig, C. *Can. J. Chem.* **1999**, *77*, 2033.

(47) Davis, M. I.; Orville, A. M.; Neese, F.; Zaleski, J. M.; Lipscomb, J. D.; Solomon, E. I. *J. Am. Chem. Soc.* **2002**, *124*, 602.

(48) EPR spectra of the complexes **1** and **2** obtained in frozen CH_3CN/acetone solution reveal different spectral pattern supporting the presence of the solid-state geometries even in solution. For **1**, the well-resolved isotropic signal near $g = 5.5$ corresponds to that predicted for a transition between the middle Kramer's doublet of monomeric high-spin iron(III) complex. A less intense signal around $g = 2.0$ is also seen. In contrast a weak signal around $g = 2.0$ is discerned for **2**; however, EPR signals (g, 6.2, 4.4, 4.0) characteristic of rhombically distorted octahedral geometry of high-spin monomeric iron(III) complex are displayed.

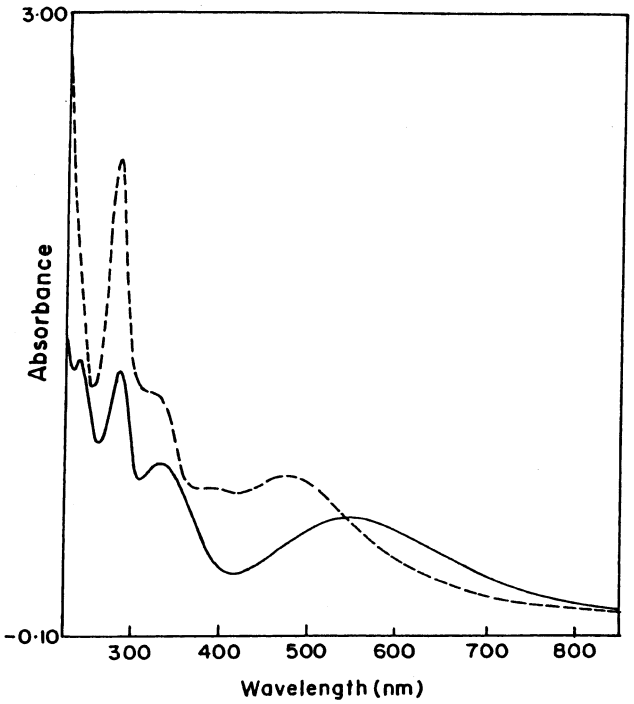

Figure 3. Electronic absorption spectra of the complexes [Fe(L1)Cl] (**1**) (---) and [Fe(L3)Cl] (**3**) (—) in acetonitrile solution. Complex concentration: **1**, 2×10^{-4} M; **3**, 2×10^{-4} M.

Electronic Absorption Spectra. The electronic absorption spectra of all the present complexes in acetonitrile solution (Figure 3) exhibit two intense bands in the near UV and one more in the visible region (Table 3). The intense absorption maximum around 365 (**2**) and 370 nm (**4**) is caused by a $\pi \rightarrow \pi^*$ transition involving nitrophenolate[40,49] units. While the high-energy band (335−430 nm) is assigned to the charge-transfer transition from the out-of-plane pπ orbital (HOMO) of the phenolate oxygen to the half-filled $d_{x^2-y^2}/d_{z^2}$ orbital of iron(III), the lowest energy band (475−550 nm) would arise from the charge-transfer transition[40,47] from the in-plane pπ orbital (POMO) of the phenolate[50] ion to the half-filled dπ^* orbital of iron(III). The shift of both these LMCT bands to lower energy is observed, on replacing the methyl groups in **1** by the electron withdrawing *p*-nitro group[40] to obtain **2**. This reflects the lower Lewis acidity of the iron center in **1** than in **2**, which is supported by the shorter and hence stronger Fe−O bonds found in **1**. The iron d-orbital energy in **1** is raised by the negative charge built[36] on Fe(III) by the stronger Fe−O(phenolate) bonds, as discussed above. It is the tripodal nature of the ligands, assisted by the electron-releasing methyl groups, which is suitable more for the novel trigonal bipyramidal coordination geometry in **1** than for the octahedral coordination geometry in **2**, as evident from the values of Fe−O−C bond angle (cf. above). Similar to **2**, the introduction of a *p*-nitro group shifts the highest energy LMCT band in **3** to lower energy in **4**; however, the low-energy LMCT band (550 nm) is shifted to higher energy (515 nm). Further, the tripodal ligand complexes **1** and **2** exhibit the LMCT band at energies higher than their respective linear ligand complexes **3** and **4**.

Significant changes in the visible band were observed (Table 4) on adding monodentate ligand molecules such as *N*-methylimidazole (mim) in excess to ensure complete adduct formation. Addition of mim and pyridine (py) shifts the band to lower energies (2−95 nm) as expected,[51] with increase in absorptivity for all the complexes, except **4**. On the other hand, addition of more basic phenolate ions effects blue shifts for all the complexes, which is expected of the stronger interaction of more basic phenolate ligands than neutral mim and py ligands; however, 2,4-di-*tert*-butylphenolate interacts weakly with **1**, possibly due to steric hindrance from the *tert*-butyl group adjacent to coordinated phenolate.

To throw light on the ability of the present complexes to interact with catechol substrates simple and sterically hindered catechols were added to them in excess (1:1.2) to ensure complete adduct formation and then their spectra were measured (Figure 4). On addition of catecholate anions to **2** and **4**, two new catecholate → Fe(III) CT bands were observed (Table 5), which are expected[21,22,52] as two different phenolate ligand orbitals are involved in the LMCT transitions. Also the high-energy band expected[51] to be blue-shifted on adduct formation would have now merged with the original PhO^- → Fe(III) CT band. The position of these bands is found to be dependent on the nature of tetradentate ligand as well as the catecholate substituents.[18−20] The blue shift of the high energy band indicates the conversion of DBC^{2-} ligand to a fairly basic ligand, which would be consistent with peroxide species in the proposed substrate activation mechanism for intradiol-cleavage mechanism.[53] The changes in spectral features observed on the addition of H_2TCC, H_2TBC, and H_2DBC (Chart 3) reflect the importance of electronic effects provided by the substituents on catechols. Thus, the lower energy absorption band is observed to shift to higher energy as the substituents on the catecholate are varied from electron-donating to electron-withdrawing ones.[54] The electron-donating *tert*-butyl groups would raise the energy of the catecholate frontier orbitals and minimize the ligand-to-metal energy gap, thus supporting the effect of methyl groups observed above in **1**. In contrast to **2** and **4**, only one catecholate-to-Fe(III) LMCT band at a

(49) Molenveld, P.; Engbersen, J. F. J.; Kooijman, H.; Spek, A. L.; Reinhoudt, D. N. *J. Am. Chem. Soc.* **1998**, *120*, 6726.
(50) MOPAC calculations (MNDO/AM1) were performed on the substituted 2-(dimethylamino)phenol.

(51) (a) Casella, L.; Gullotti, M.; Pintar, A.; Messouri, L.; Rockenbauer, A.; Gyor, M. *Inorg. Chem.* **1987**, *26*, 1031. (b) Krebs, B.; Schepers, K.; Bremer, B.; Henkel, G.; Althus, E.; Muller-Warmuth, W.; Griesar, K.; Haase, W. *Inorg. Chem.* **1996**, *35*, 2360. (c) Wang, S.; Wang, L.; Wang, X.; Luo, Q. *Inorg. Chim. Acta* **1997**, *254*, 71.
(52) (a) Cox, D. D.; Que, L., Jr. *J. Am. Chem. Soc.* **1988**, *110*, 8085. (b) Salama, S.; Stong, J. D.; Neilands, J. B.; Spiro, T. G. *Biochemistry*, **1978**, *17*, 3781. (c) Koch, W. O.; Kruger, H.-J.; *Angew. Chem., Int. Ed. Engl.* **1997**, *36*, 1342. (d) Lim, J. H.; Lee, H.-J.; Lee, K.-B.; Jang, H. G. *Bull. Korean. Chem. Soc.* **1997**, 18, 1166.
(53) (a) Lipscomb, J. D.; Orville, A. M. *Met. Ions Biol. Syst.* **1992**, *28*, 243. (b) Que, L., Jr.; Ho, R. Y. N. *Chem. Rev.* **1996**, *96*, 2607. (c) Que, L., Jr. In *Bioinorganic Catalysis*, 2nd ed.; Reedijk, J., Bouwman, E., Eds.; Marcel Dekker: New York, 1999; p 269.
(54) (a) Whittaker, J. K.; Lipscomb, J. D.; Kent, T, A.; Munck, E. *J. Biol. Chem.* **1984**, *259*, 4466. (b) Que, L., Jr.; Heistand, R. H., II. *J. Am. Chem. Soc.* **1979**, *101*, 2219. (c) Felton, R. H.; Barrow, W. L.; May, S. W.; Sowell, A. L.; Goel, S.; Bunker, G.; Stern, E. A. *J. Am. Chem. Soc.* **1982**, *104*, 6132.

Table 3. Electronic Spectral Data[a] for Iron(III) Complexes and Their Adducts in CH_3CN

	λ_{max}, nm (ϵ, M^{-1} cm^{-1})			
added ligand[b]	[Fe(L1)Cl] (**1**)	[Fe(L2)(H_2O)Cl] (**2**)	[Fe(L3)Cl] (**3**)	[Fe(L4)Cl] (**4**)
none	475 (4000)	515 (3530)	550 (2820)	515 (4860)
	335 (6150)	430 (5510)	340 (4360)	425 (8250)
	285 (13 225)	365 (15 970)	285 (7185)	370 (16 685)
H_2CAT[c]	475 (4120)	660 (3100)	465 (2515)	645 (2055)
	285 (15 630)	410 (25 750) (sh)	350 (2865) (sh)	400 (24 155)
		380 (29 430)	285 (9845)	295 (7515)
		300 (10 210)	245 (11 900)	
H_2DBC	540 (4530)	700 (1560)	545 (2670)	690 (2015)
	290 (16 065)	410 (14 780) (sh)	470 (2480) (sh)	410 (25 000)
		390 (16 360)	375 (2540) (sh)	300 (7600)
		300 (6915)	300 (10 535)	
H_2TBC	485 (4180)	685 (3270)	475 (2500)	675 (2175)
	335 (6535) (sh)	410 (25 800) (sh)	350 (3030) (sh)	410 (24 550)
	280 (17 000)	380 (30 170)	300 (9410) (sh)	285 (8200)
		300 (10 770)	285 (11 160) (sh)	
H_2TCC	495 (5785)	580 (3725)	495 (3960)	410 (17 395)
	295 (14 670)	415 (17 370) (sh)	300 (10 890)	365 (15 639)
		370 (11 995)		315 (10 390)
		310 (17 375) (sh)		

[a] Concentration of iron complexes $\times$ 10^{-4} M. [b] The ratio of added ligands to iron complexes was 1:1; the anions were generated by adding 2 equiv of triethylamine. [c] H_2DBC = 3,5-di-*tert*-butylcatechol; H_2TBC = 4-*tert*-butylcatechol; H_2CAT = catechol; H_2TCC = tetrachlorocatechol.

Table 4. Spectral Data for the Interaction of Iron(III) Complexes[a] with Monodentate Bases in CH_3CN Solution

	λ_{max}, nm (ϵ, M^{-1} cm^{-1})			
added ligand[b]	[Fe(L1)Cl] (**1**)	[Fe(L2)(H_2O)Cl] (**2**)	Fe(L3)Cl] (**3**)	[Fe(L4)Cl] (**4**)
none	475 (4000)	515 (3 530)	550 (2820)	515 (4860)
	335 (6150)	430 (5510)	340 (4360)	425 (8250)
	285 (13 225)	365 (15 980)	285 (7185)	370 (16 685)
mim[c]	570 (4960)	515 (3409)	570 (3845)	515 (5160)
	340 (4885)	415 (5320)	345 (2815)	415 (7200)
	290 (11 930)	350 (14 345)	285 (8040)	350 (14 601)
py	565 (4165)	515 (3620)	565 (3610)	515 (5100)
	330 (5500)	420 (5215)	340 (3570)	420 (7355)
		360 (14 920)		360 (16 095)
p-Cl-PhO^-	465 (6475)	490 (4475)	465 (4010)	490 (5910)
	330 (7200)	405 (16 185)	335 (4500)	415 (23 300)
		375 (16 285)		370 (15 935)
DBP^{2-}	495 (4365)	495 (3190)	430 (2180)	490 (2555)
	325 (7015)	420 (8235)	335 (4815)	370 (18 115)
		370 (15 490)	280 (21 990)	275 (20 490)

[a] Concentration of the complexes: 1.5 $\times$ 10^{-4} M. [b] The ratio of added ligands to iron complexes was 10:1; the anions were generated by adding 1 equiv of triethylamine. [c] mim = 1-methylimidazole; py = pyridine; *p*-Cl-PhO^- = *p*-chlorophenolate; H_2DBP = 2,4-di-*tert*-butylphenol.

lower energy (475−540 nm) is obtained for **1** on the addition of catecholates. Also, the trend observed in the position of the band reflects the steric crowding and electronic effects provided by the catechols on binding to **1**. Further, for **3** also only one but blue-shifted (5−85 nm) LMCT band is observed. This is interesting in view of the failure of **1** and **3** to catalyze the intradiol cleavage (cf. below).

Redox Properties. The redox behavior of the present iron(III) chloride complexes were investigated using cyclic voltammetry (CV) and differential pulse voltammetry (DPV) on a stationary platinum sphere electrode. All the complexes show a cathodic wave (−0.244 to −0.660 V, Table 6). The i_{pc} vs $v^{1/2}$ plot for 0.01−0.50 V/s scan rates is linear, suggesting a diffusion-controlled reduction process and the values of the diffusion coefficients calculated by assuming reversibility (D, 1.5−3.5 $\times$ 10^{-6} cm^2/s) are of the same order as those observed for other iron(III) complexes.[25] Only the complexes **2** and **4** show the corresponding anodic wave (**2**, −0.160; **4**, −0.308 V); the values of i_{pa}/i_{pc} (**2**, 1.0; **4**, 0.9) and peak potential separation ΔE_p (**2**, 84 mV; **4**, 92 mV) suggest a fairly chemically reversible redox process (i_{pa}/i_{pc} = 1 for Nernstian redox process and ΔE_p = 59 mV for reversible heterogeneous electron transfer). In contrast, the five-coordinate complexes **1** and **3** are completely chemically irreversible as evident from the absence of the corresponding anodic wave. The $E_{1/2}$ values for Fe^{III}/Fe^{II} couple exhibit the following trends: Fe(L1) < Fe(L2), Fe(L3) < Fe(L4). This reflects the increase in Lewis acidity of the iron(III) center as the electron-releasing methyl groups on the phenolate donors are replaced by the *p*-NO_2 group. The trend in Lewis acidity for **1** and **2** is consistent with that derived from PhO^- → Fe(III) LMCT band energies. Interestingly, the redox potentials of linear ligand complexes **2** and **4** are more negative than the respective tripodal ligand complexes **1** and **3**. This is consistent with the trend observed in the energies of LMCT bands and suggests that linear ligands are more suitable than tripodal ligands to strongly bind to and hence confer decreased Lewis acidity on the iron(III) center.

The cyclic and differential pulse (Figure 5) voltammetric results for $[Fe(L)DBC]^-$ adducts generated in situ, as

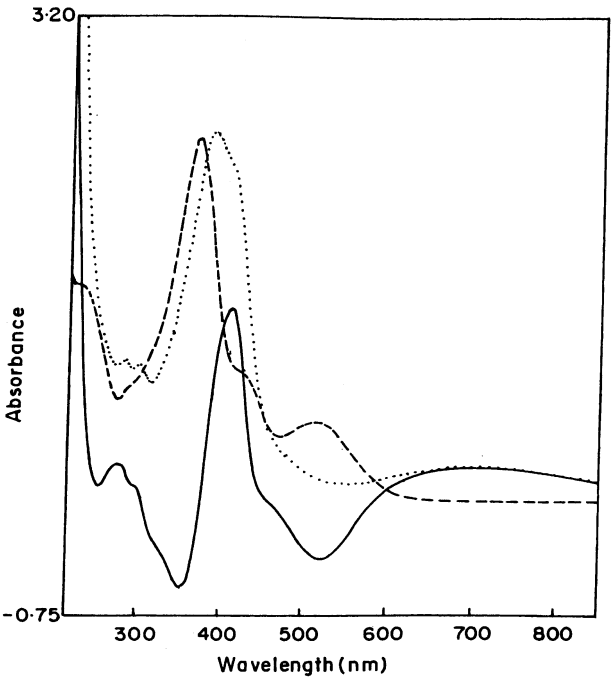

Figure 4. Absorption spectra (vs acetonitrile) of [Fe(L2)(H_2O)Cl] (**2**) (---) [Fe(L2)(DBC)]$^-$ (···) and difference spectra of [Fe(L2)(DBC)]$^-$ vs [Fe(L2)(H_2O)Cl] (—) in acetonitrile solution.

evidenced by spectral measurements, are collected in Table 6. The redox potentials of the DBSQ/DBC couple[55] (**1**, −0.313 V; **2**, −0.101 V; **3**, −0.395 V; **4**, −0.189 V) are significantly more positive than that (−1.434 V, Ag/Ag^+)[56] of free H_2DBC, reflecting the considerable stabilization of H_2DBC by chelation to iron(III). They are more positive than, and display the same trend as, that of the Fe^{III}/Fe^{II} couple of the parent complexes. They also reflect[57] the Lewis acidity of the iron center in DBC^{2-} adducts, which decreases on replacing the *p*-nitro substituent by dimethyl substituents on the phenolate ring. Also they are more positive than those for [Fe(salen)DBC]$^-$ (−0.179 V, NHE)[58] and [Fe(NTA)-DBC]$^{2-}$ (−0.024 V, NHE)[57] adducts, which exhibit catechol cleavage activity. This implies that all the present complexes should show cleavage activity. However, the shifts in the redox potential of the DBSQ/DBC couple of **1**−DBC^{2-} and **3**−DBC^{2-} adducts are less negative suggesting monodentate or weaker coordination of DBC^{2-} and hence no cleavage activity for these complexes; this is supported by the very small or negligible changes in Fe^{III}/Fe^{II} redox potentials and $PhO^- \rightarrow$ Fe(III) LMCT bands on adduct formation. Further, the coordination of DBC^{2-} depresses the redox potential of the Fe^{III}/Fe^{II} couple (**2**, 320 mV; **3**, 250 mV; **4**, 420 mV) reflecting the decrease in Lewis acidity of the iron center on substrate binding. This supports the suggestion that the iron(III) center in the dioxygenases not only participates in the activation of the substrate but also facilitates the latter stages of the reaction, like dissociation of the product. The appearance of the $DBC^{2-} \rightarrow$ Fe(III) LMCT band and DBSQ/DBC redox wave and the lowering of the Fe(III)/Fe(II) redox potential on adding H_2DBC, even in the absence of added base, illustrate the spontaneous deprotonation of the later on binding to iron(III).

Study of Catechol 1,2-Dioxygenase Activity. The catechol-cleaving dioxygenase activity[11,12,36] of the present complexes toward 3,5-di-*tert*-butylcatechol (H_2DBC) was examined by exposing to dioxygen a DMF solution of the iron(III) complex−DBC^{2-} adducts generated in situ by treating the complexes with H_2DBC and piperidine and monitoring the disappearance of the low-energy LMCT band (Figure 6) at ambient temperature. The oxygenated products were identified using GC-MS analysis. From the reaction mixture two intradiol [$C_{14}H_{20}O_3$, 61%, *m*/*z* 236 (M^+); 3,5-di-*tert*-butyl-1-oxacyclohepta-3,5-diene-2,7-dione (**A**), $C_{15}H_{24}O_4$, 25%, *m*/*z* 267 (M^{2+}); 3,5-di-*tert*-butyl-5-(*N*,*N*-dimethylamidomethyl)-2-furanone (**B**), which is the product of dimethylamine attack on the anhydride **A**] and one extradiol [3,5-di-*tert*-butyl-2-pyranone (**C**), $C_{13}H_{20}O_2$, 14%, *m*/*z* 208 (M^+)] cleavage product (Scheme 1) were identified for **2**. In contrast, interestingly, only one intradiol cleavage product (**A**) was identified for **4**.

A plot of [1 + log(abs)] vs time is linear for complex **2** suggesting a pseudo-first-order kinetics. The rate of the reaction calculated for **2** using the equation

$$k_{O_2} = k_{obs}/[O_2]$$

is 3.76×10^{-3} M^{-1} s^{-1}. As **4** reacts very fast, no attempt was made to measure the rate. As proposed by Que et al., the reactivity of iron(III)−catecholate adduct with O_2 would correlate with the Lewis acidity of the iron(III) center. A decrease in Lewis acidity of the iron(III) center decreases the covalency of the iron−catecholate interaction, the semiquinone character of bound DBC^{2-}, and hence the reaction rate. Thus, the iron(III) complex **4** with a Lewis acidity lesser than **2** (cf. above) would be expected to exhibit a lower rate of dioxygenase reaction. However, interestingly, **4** reacts much faster[18] than **2**. Unlike the tripodal ligand complex **2**, the linear tetradentate ligand in **4** should rearrange itself to provide cis-coordination positions for bidentate coordination of the catechol substrate. The increased steric congestion and the enhanced negative charge built on iron(III) in **4**−DBC^{2-} compared to **2**−DBC^{2-} adduct would facilitate the rate-determining product releasing phase in the reaction mechanism proposed by Que et al. for intradiol-cleaving dioxygenases. We have made similar observations previously[26] for bis(phenolate) ligand complexes. Also it is relevant to note that the reactivities of iron(III) complexes of tetradentate tripodal ligands differ from those of tetradentate macrocyclic ligands.[59] Further, it is interesting that only **2** yields the extradiol product **C**; so far only a few examples of synthetic iron complexes[22,60,61] capable of carrying out extradiol-

(55) Johnson, C. R.; Henderson, W. W.; Shepherd, R. F. *Inorg. Chem.* **1984**, *23*, 2754.
(56) Nanni, E. J.; Stalling, M. D.; Sawyer, D. T. *J. Am. Chem. Soc.* **1980**, *102*, 4481.
(57) White, L. S.; Nilsson, L. H.; Pignolet, L. H.; Que, L., Jr. *J. Am. Chem. Soc.* **1984**, *106*, 8312.
(58) Lauffer, R. B.; Heistand, R. H., II.; Que, L., Jr. *J. Am. Chem. Soc.* **1981**, *103*, 3947.
(59) Dei, A.; Gatteschi, D.; Pardi, L. *Inorg. Chem.* **1993**, *32*, 1389.
(60) Pyrz, J. W.; Roe, A. L.; Stern, L. J.; Que, L., Jr. *J. Am. Chem. Soc.* **1985**, *107*, 614.

Table 5. LMCT Spectral Data[a] for DBC^{2-} Adducts of Iron(III) Complexes in CH_3CN

	λ_{max}, nm (ϵ, M^{-1} cm^{-1})			
added ligand[b]	[Fe(L1)Cl] (**1**)	[Fe(L2)(H_2O)Cl] (**2**)	[Fe(L3)Cl] (**3**)	[Fe(L4)Cl] (**4**)
None	475 (4000)	515 (3530)	550 (2820)	515 (4860)
	335 (6150)	430 (5510)	340 (4360)	425 (8250)
	285 (13 225)	365 (15 980)	285 (7185)	370 (16 685)
DBC^{2-} vs complex	595 (2595)	700 (1555)	805 (195)	695 (1965)
	400 (−588)	520 (−2480)	545 (−325)	520 (−3490)
	360 (1085)	410 (8550)	425 (920)	450 (−1245)
	300 (8480)	355 (−3760)	350 (−840)	410 (15 997)
	276 (−671)	275 (1590)	300 (5325)	355 (−3560)
DBC^{2-} vs CH_3CN	540 (4530)	700 (1560)	545 (2670)	690 (2015)
	460 (3865) (sh)	410 (14 880) (sh)	470 (2480) (sh)	410 (25 000)
	290 (16 065)	390 (16 360)	375 (2540) (sh)	300 (7600)
			300 (10 100)	

[a] Concentration of iron(III) complexes: 1.5×10^{-4} M. [b] The catecholate anions were generated by adding 2 equiv of triethylamine to solutions containing the catechol and the iron complex in a 1:1 ratio.

Table 6. Electrochemical Data[a] for the Parent and DBC^{2-}-Bound Complexes[b] $[Fe(L)DBC]^-$ in Methanol at 25 ± °C Using a Scan Rate of 50 mV/s

				$E_{1/2}$ (V)		
compd	E_{pc} (V)	E_{pa} (V)	ΔE_p (mV)	CV	DPV[c]	redox process
[Fe(L1)Cl]	−0.600	−0.390	210	−0.495	−0.483	$Fe^{III} \rightarrow Fe^{II}$
$[Fe(L1)DBC]^-$ [d]	−0.386	−0.254	158	−0.320	−0.313	DBSQ → DBC
		0.592			0.637	DBQ → DBSQ
[Fe(L2)(H_2O)Cl]	−0.244	−0.160	84	−0.202	−0.205	$Fe^{III} \rightarrow Fe^{II}$
$[Fe(L2)DBC]^-$	−0.488				−0.525	$Fe^{III} \rightarrow Fe^{II}$
	−0.122	−0.026			−0.101	DBSQ → DBC
		0.630			0.627	DBQ → DBSQ
[Fe(L3)Cl]	−0.660				−0.581	$Fe^{III} \rightarrow Fe^{II}$
$[Fe(L3)DBC]^-$	−0.750				−0.833	$Fe^{III} \rightarrow Fe^{II}$
	−0.450	−0.338	112	−0.394	−0.395	DBSQ → DBC
		0.782			0.720	DBQ → DBSQ
[Fe(L4)(H_2O)Cl]	−0.400	−0.308	92	−0.354	−0.345	$Fe^{III} \rightarrow Fe^{II}$
$[Fe(L4)DBC]^-$	−0.530				−0.763	$Fe^{III} \rightarrow Fe^{II}$
	−0.232	−0.150	82	−0.191	−0.189	DBSQ → DBC
					0.650	DBQ → DBSQ

[a] E in volts vs $Ag/AgNO_3$ (0.01 M, 0.1 M TBAP); add 0.544 V to convert to NHE. [b] Generated by adding to complex 1 and 2 equiv of H_2DBC and triethylamine, respectively. [c] Pulse height: 25 mV. [d] Difficult to discern Fe(III)/Fe(II) couple.

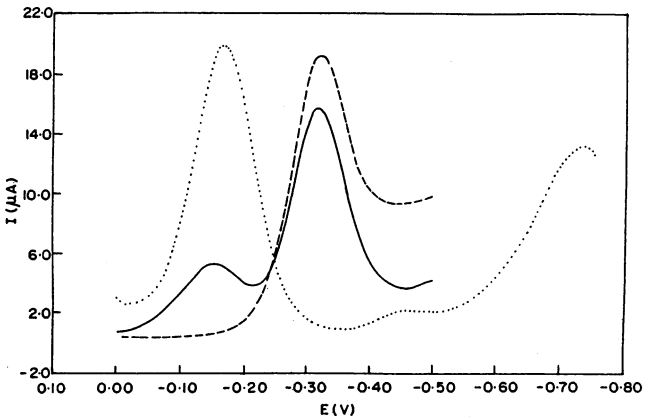

Figure 5. Differential pulse voltammograms of 1 mM [Fe(L4)(H_2O)Cl] (**4**) (•••), with 1 mM H_2DBC added (—) and 2 mM triethylamine (---) added in methanol at 25 °C. Supporting electrolyte: 0.1 M TBAP. Scan rate: 1 mV s^{-1}.

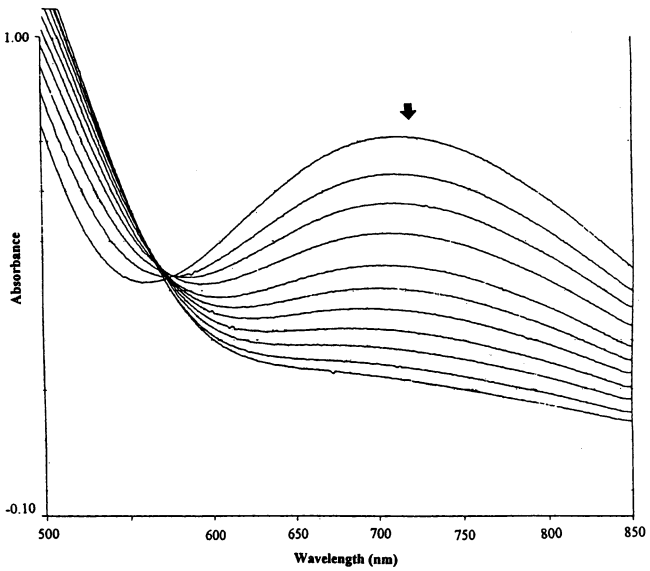

Figure 6. Progress of the reaction of $[Fe(L2)(DBC)]^-$ with O_2 in DMF solution. The disappearance of the catecholate-to-iron(III) charge-transfer band was monitored.

cleavage are known in the literature. We have very recently reported that 1:1 iron(III) complexes[62] of tridentate ligands catalyze both intra- and extradiol cleavage of H_2DBC in the presence of dioxygen.

Conclusions and Relevance to Iron Oxygenases. A few bis(phenolato)iron(III) complexes of new tetradentate tripodal/linear N_2O_2 ligands comprising of different substituents at positions *ortho* and *para* to the phenolic oxygen atom have

(61) Ito, S.; Suzuki, M.; Kobayashi, T.; Itoh, H.; Harada, A.; Ohba, S.; Nishida, Y. *J. Chem. Soc., Dalton Trans.* **1996**, 2579.
(62) Velusamy, M.; Palaniandavar, M. *J. Chem. Soc., Dalton Trans.*, submitted for publication.

Scheme 1

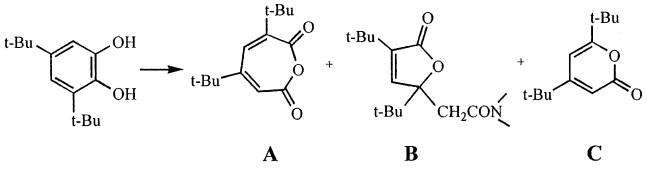

been isolated and studied as structural and functional models for catechol dioxygenases. On replacement of the *p*-NO_2 group on the coordinated phenolate ring by 2,4-dimethyl groups, a remarkable change in the iron(III) coordination geometry from distorted octahedral to trigonal bipyramidal is observed, which is accompanied by interesting changes in the spectral and electrochemical properties of the complexes. It is noteworthy that the trigonal bipyramidal coordination geometry of the synthetic complexes bears a close resemblance to that of CTD enzyme active site; however, most importantly, these complexes fail to elicit catechol 1,2-dioxygenase activity. To throw light on these interesting observations a spectral and electrochemical study on the interaction of the present complexes with simple and substituted catechols was undertaken.

When simple and substituted catechols are added to the present octahedral iron(III) complexes two broad catecholate → Fe(III) LMCT bands are observed, which is typical of bidentate coordination of catechols as also observed previously for other octahedral iron(III) complexes.[18−22] The broad low-energy band strikingly resembles the one exhibited by the substrate complexes of PCD or CTD enzyme in steady-state conditions. Further, the position of the higher energy band follows the order of electron-donating and electron-withdrawing effects of substituents on catechol as expected. As revealed by its X-ray crystal structure, the tripodal ligand complex makes available cis-coordination positions for the binding of bidentate catechols. On the other hand, the linear tetradentate ligand complex should rearrange to accommodate the bidentate catechols. Thus, the binding of catechol substrate to the octahedral complexes is expected to occur without replacing the already bound donors. The changes in the high-energy absorption band in the octahedral complexes are then ascribed to structural changes accompanying binding of H_2DBC and/or to the overlap of CAT^{2-} → Fe(III) CT bands with phenolate → Fe(III) CT bands. Further, the observation of the DBC^{2-} → Fe(III) LMCT band and DBSQ/DBC redox wave and the lowering of the Fe(III)/Fe(II) redox potential on adding H_2DBC, even in the absence of added base, demonstrate the spontaneous deprotonation of the later on binding to iron(III). This is consistent with one of the suggested functions of the iron center in the enzyme, viz., promoting the loss of both protons of the substrate. Also this is relevant to the observation that the presence of catechol lowers the potential of the iron(III) center in the enzyme and renders it difficult to reduce under biological conditions. We have made similar observations previously.[25,26]

In contrast to the six-coordinate complexes, only one higher energy catecholate → Fe(III) LMCT band (475−550 nm) is observed for the five-coordinate complexes on adding simple and substituted catechols; however, the changes in spectral features observed reflect the importance of electronic effects provided by the substituents on catechols. This is consistent with the failure of the complexes to catalyze the intradiol cleavage. It appears that the catechols are involved in monodentate rather then bidentate coordination; the latter is essential for intradiol cleavage to occur, as illustrated in the substrate activation mechanism proposed[53] by Que et al. In fact, recent structures[63] of protocatechuate 3,4-dioxygenase (PCD) enzyme cocrystallized from substrate analogues have demonstrated that the axial tyrosine ligand, Tyr-447, swings away from the iron(III) center upon binding of substrate analogues, leaving only three amino acid ligands for the iron(III) center.

To conclude, this study shows that suitably tailored—sterically hindered and strongly Lewis basic—bis(phenolate) ligands can stabilize five-coordinate iron(III) geometries that closely mimic the active site geometry of the intradiol-cleaving enzymes and confer interesting spectral and chemical properties. A noteworthy observation is that the substituents on the bis(phenolate) ligands lead to tune the Lewis acidity of the iron(III) center and hence determine the course and products of dioxygenase activity of the complexes, thereby providing support to the substrate activation mechanism of intradiol cleavage.[53] We have very recently shown[62] that the rate of dioxygenase reaction is dependent upon the Lewis acidity of the iron(III) center, steric demand, and the presence of hydrogen-bonding functionalities in tridentate ligand complexes. To elucidate the electronic and steric effect of substituents *ortho* to the phenolate donors on the ring cleavage pattern detailed characterization and study of dioxygenase activity of iron(III) complexes of differently substituted bis(phenolate) ligands are in progress.

Acknowledgment. We sincerely thank the Department of Science and Technology, New Delhi, for supporting this research (Scheme No. S1/IC/01) and the Council of Scientific and Industrial Research, New Delhi, for a Senior Research Fellowship to M.V. We thank Professor C. N. R. Rao, FRS, Jawaharlal Nehru center for Advanced Scientific Research, for kindly providing the diffractometer facility.

Supporting Information Available: A description of the structure of the ligand H_2(L1), a ZORTEP drawing of H_2(L1), EPR spectra, and tables of the final atomic coordinates of non-hydrogen atoms, complete bond lengths and bond angles, anisotropic thermal parameters for non-hydrogen atoms, and atomic coordinates for hydrogen atoms for H_2(L1), **1**, and **2**. This material is available free of charge via the Internet at http://pubs.acs.org.

IC020569W

(63) Orville, A. M.; Lipscomb, J. D.; Ohlendorf, D. H. *Biochemistry* **1997**, *36*, 10052.